Simulation of an aperture for the EXL experiment at the ESR

Mirko von Schmid
March 16, 2012, v2.0

TECHNISCHE UNIVERSITÄT DARMSTADT

FAIR GSI KVI HIC for FAIR Helmholtz International Center Bundesministerium für Bildung und Forschung

Contents

1 Introduction

This document summarizes the results of my simulations for a slit aperture for the gas-jet target at the ESR. The simulation is based on calculations of LISE++ 9.3 (parametrizations of elastic and inelastic scattering, energy loss in matter) and Mathematica 8.0 (random-number generator). The simulations were performed to get a first impression of the leading-order effects of a slit aperture and to fix the rough dimensions of it in order to improve the angular resolution of the measurement. My simulations should be checked with GEANT4 simulations later on.

1.1 Description of the Simulation

To get a better understanding of the features and limitations of my simulation I will briefly explain it step by step:

1. An interaction point between beam and target is chosen. Therefore a 2D gaussian-beam profile is overlayed with a 2D gaussian profile of the gas-jet target and the random number is chosen according to the resulting probability distribution. The point of interaction is given realtive to the reference point $(0, 0, 0)$.

2. At the interaction point a random angle is chosen as a result of elastic or inelastic scattering which took place at the interaction point.

3. The parameterisations of the kinematics are used to get the energy to the corresponding scattering angle.

4. The angle of the recoil at the slit plane is calculated realtive to the reference point. If it is indicated that the particle would colide with the slit plate, the energy loss is calculated based on a parametrisation by LISE++.

5. The same procedure takes place for the DSSD and the two following SiLi detectors. The energy losses are summed up then and the resulting value is randomized according to the energy resolution at this energy.

6. Histograms are filled if the recoil wasn't fully stopped in the slit. At the same time counters for statistical useage are increased.

1.2 Limitations of the Simulation

In comparism to more sophisticated approaches like GEANT4 my simulations is subject to several limitations. The most obvious ones are (with the same numbering as in 1.1):

1. There is no real interaction of particles and therefore the probability distribution might not be precise. The beam doesn't have an energy distribution either.

2. The cross-section is constant for all angles and equal for elastic and inelastic scattering.

3. $\cdots$

4. I'm projecting all events to a plane (i.e. no ϕ angle). The detectors have zero thickness, so that the energy loss takes place instantly and hence the edge effects at the slit or the detectors are not simulated. Last but not least, I don't consider energy or angular straggling and while the energy loss in the detectors is parameterized for an incident angle of $90° \pm 10°$ the energy loss in the slit is parameterised for 90° only.

5. The energy resolution is applied to the whole detector stack as a total. See chapter 2.3 for more information.

6. ...

2 Input

2.1 Gemoetry

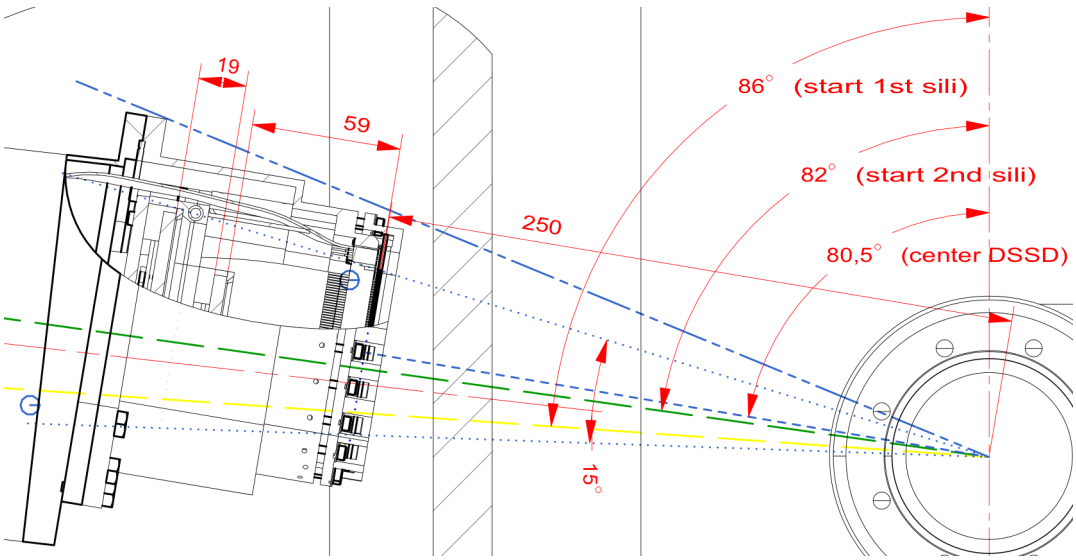

Figure 1: Schematics of the geometry used for the simulations (Drawing by M. Lindemulder)

The geometry is based on a drawing of Michel Lindemulder found at the EXL wiki (last checked 17.02.2012, see also fig 1). The numbers which were used in the simulation can be found in table 1. Values which are marked with a star are calculated ones.

2.2 Physical parametrisations

The kinematic curves for elastic and inelastic scattering are calculated with LISE++ for the case of ^{56}Ni(p,p)^{56}Ni and ^{56}Ni(p,p)^{56}Ni with 400 MeV/u beam energy each. For the inelastic scattering the first excited states (^{56}Ni: 2700.6 keV, ^{58}Ni: 1454.21 keV) were used. The energy losses are calculated with LISE++ as well for 285 μm Si (DSSD), 6.5 mm Si (SiLi) and stainless steel of 3 mm, 4 mm and 5 mm thickness (slit). All these tables are then imported into Mathematica and interpolated (first-order interpolation).

2.3 Energy resolution

To estimate the energy resolution of the detector system I have used measured values from recent experiments (see table 2). These values are interpolated and then used to randomize the value of the total measured energy.

3 Results

3.1 Without slit

The first figure (fig. 2) shows the situation without a slit for ideal (fig. 2 a)) and more realistic conditions (fig. 2 b)). To simulate an ideal beam/target I have set the width of each to 0.1 mm FWHM. The grey boxes indicate the angular coverage and the maximum energy loss of each of the three detectors. It has to be mentioned that the maximum energy loss is calculated for the case that the particle went through its the previous detector(s).

To show the way how elastic and inelastic scattering do overlay each other I have seperated the channels from each other and plotted them color coded in figure 3.

beam	
beam vector	$(1, 0, 0)$
width (FWHM)	3.1 mm
target	
target vector	$(0, 0, 1)$
width (FWHM)	5.5 mm
slit	
material	stainless steel
thickness	variable
slit size	variable
width	variable
distance	variable
normal angle	80.5°
DSSD	
material	Silicon
thickness	285 μm
width	64 mm
strip pitch	500 μm
distance	250 mm
normal angle	80.5°
SiLi 1	
material	Silicon
thickness	6.5 mm
width	50 mm
start angle	86°
stop angle*	76.8°
distance	309 mm
normal angle	80.5°
SiLi 2	
material	Silicon
thickness	6.5 mm
width	50 mm
start angle	82°
stop angle*	73.5°
distance	334.5 mm
normal angle	80.5°

Table 1: Common input values as used in the simulation

3.2 Distance to the target and slit size

To determine the approximate distance of the aperture to the target and the opening width of the slit four simulations were performed. While keeping the slit infinitely thick and fairly wide (1 m) the distance d was set to 10 mm or 20 mm and the slit opening to 1 mm or 2 mm. The results can be found in figure 4. In terms of angular resolution all four configurations would be acceptable to seperate the elastics from the inelastics. To verify that the channels are really seperated by each other I have ploted them color coded again in figure 5.

When comparing the several simulations one notes a deviation of the simulated kinematic curves from the theoretical curves which increase for bigger distances (while it is absent for the point-like beam). This is illustrated in figure 6 where the measured angle (i.e. the strip at the DSSD) is plotted vs. the real angle given by the random-number generator.

A big issue is the loss of rate due to the slit. In table 3 the percentage of events registered in the DSSD is given relative to the case without slit (fig. 2 a)).

3.3 Thickness of the slit plate

For the case of a 1 mm slit in a distance of 10 mm away from the target three simulations with slits of 3 mm, 4 mm and 5 mm stainless steel were performed. The results are plotted in figure 7 together with a simulation of an infinite thick slit as a reference. A 5 mm thick slit seems to be thick enough to stop all protons up to the point where the range of the first Si(Li) ends.

Energy	Resolution (FWHM)	Remarks
0 MeV	100 %	“Noise“, extrapolation
0.07 MeV	40 %	p, Tübingen
1.5 MeV	1 %	p, Tübingen
5.5 MeV	0.4 %	α, new DSSD
50 MeV	0.7 %	p, 1. demonstrtor @ KVI
135 MeV	0.7 %	p, 2. demonstrtor @ KVI
400 MeV	0.7 %	extrapolation

Table 2: Estimated resolution of the detector system

	$d = 10$ mm	$d = 20$ mm
$s = 1$ mm	16.8 %	15.0 %
$s = 2$ mm	37.7 %	29.7 %

Table 3: Remaining statistics in the DSSD for different distances d and slit sizes s relative to fig. 2 a)

3.4 Width of the slit plate

To estimate the outer width of the slit which will be needed to shield the DSSD from all unwanted events I have performed four simulations with two different widths of the plate (10 mm and 20 mm) in two distances (10 mm and 20 mm). The results are shown in figure 8. It seems like that already a 20 mm wide plate seems to be enough.

3.5 Comparism with ^{58}Ni

Finally in figure 9 I have simulated a 1 mm slit of 20 mm width and a thickness of 5 mm stainless steel together with a ^{58}Ni beam and compared the results with the corresponding ^{56}Ni data. Since the first excited state of ^{58}Ni is lower than the one of ^{56}Ni the seperation of the lines is worse. In figure 10 cuts for several angles (78°, 81°, 84°) are shown.

4 Conclusions

The simulations show that the slit plate should be at least 20 mm wide and be made of 5 mm stainless steel. A distance of 10 mm to the target should be aimed for. This setup will offer sufficient angular resolution to seperate the kinematic curves even for ^{58}Ni. However the rate drops almost by an order of magnitude. Finally, figure 11 shows the final setup (colored) on top of the original situation without a slit.

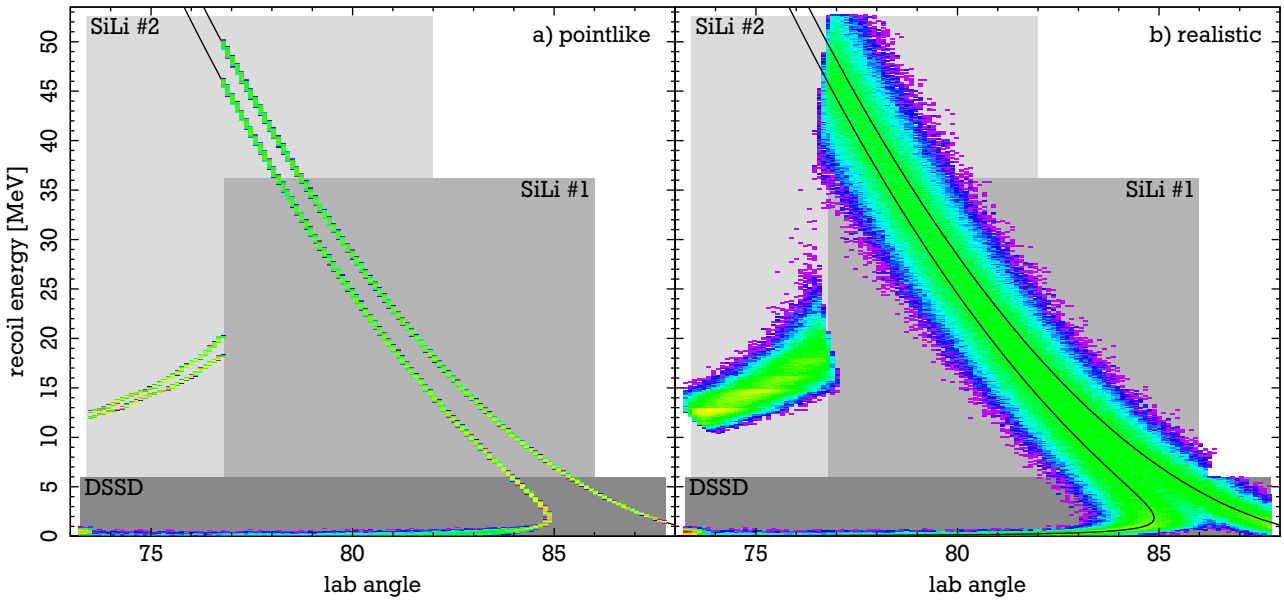

Figure 2: a) pointlike beam and target, no slit; b) realistic beam and target distribution, no slit

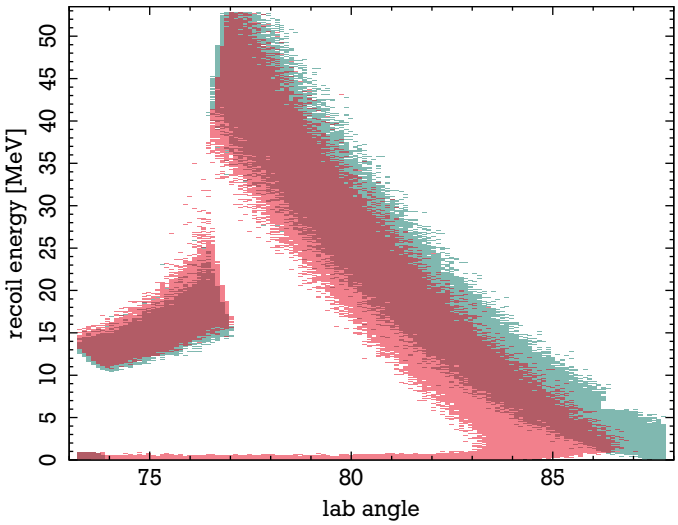

Figure 3: Simulation without a slit; green: elastic scattering; red: inelastic scattering

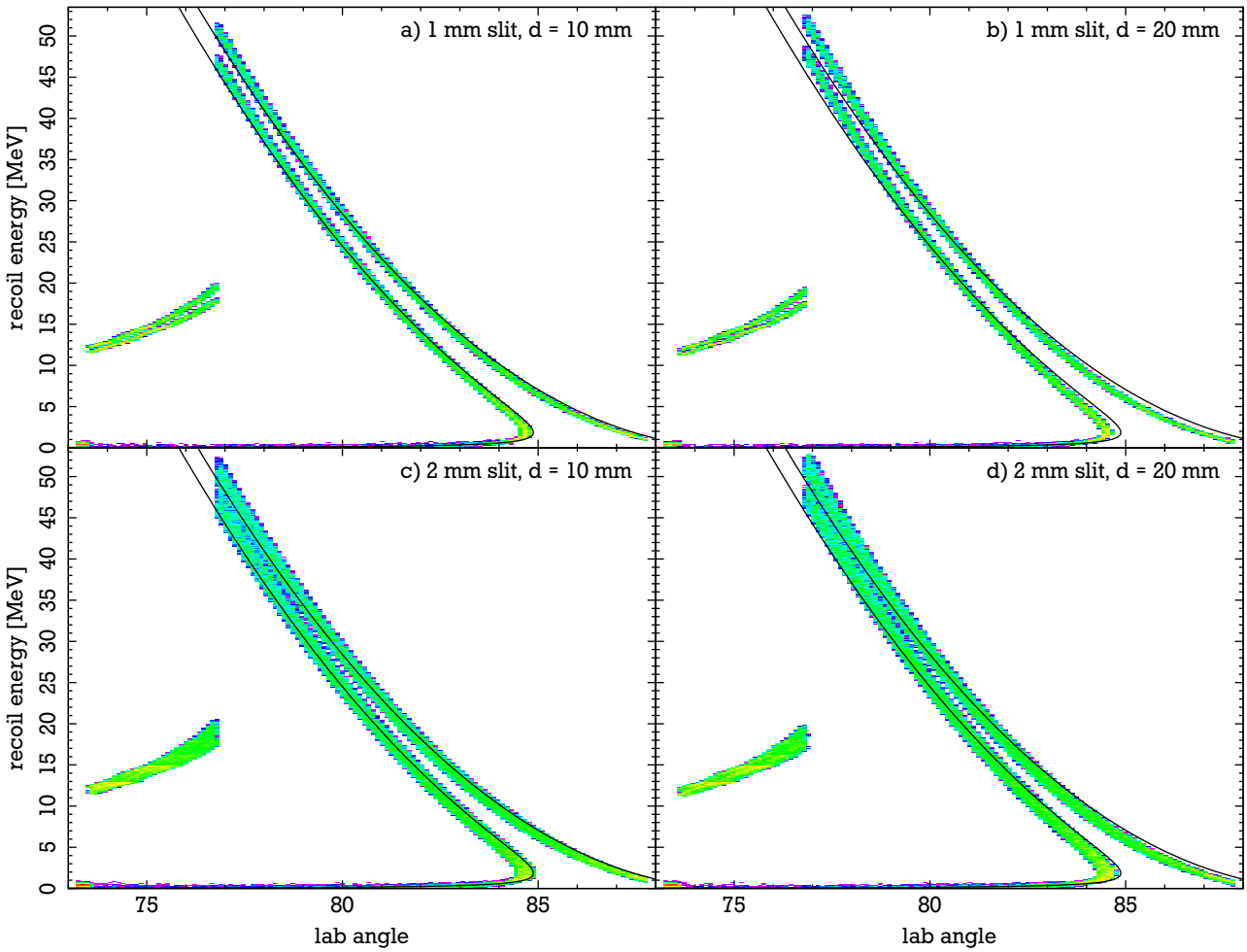

Figure 4: Simulations to determine distance d and size of the slit

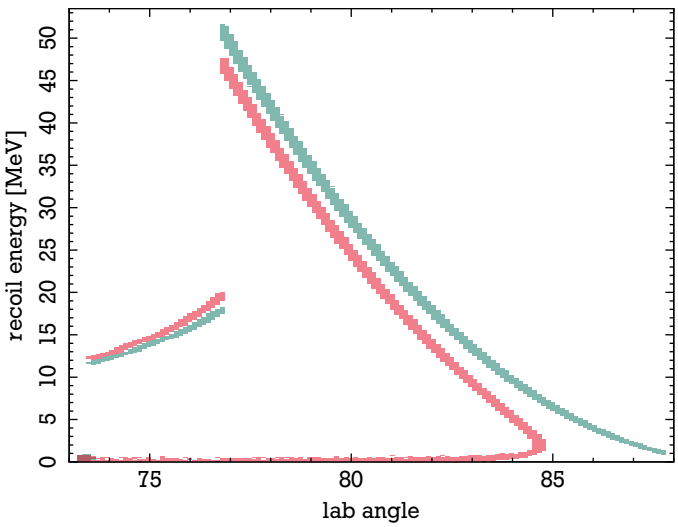

Figure 5: Simulation with a 1 mm slit at 10 mm distance; green: elastic scattering; red: inelastic scattering

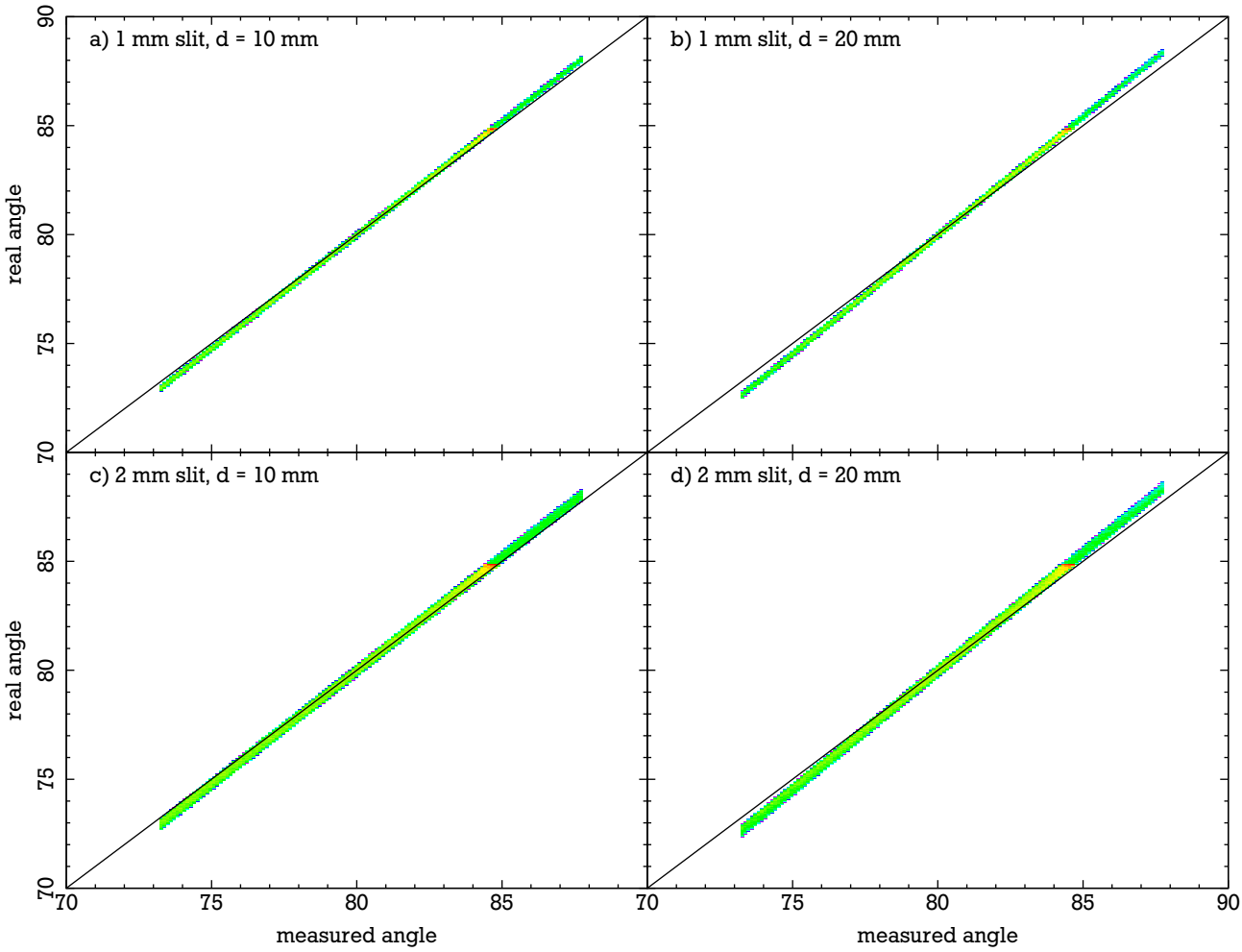

Figure 6: Corelations of measured angles vs. real angles

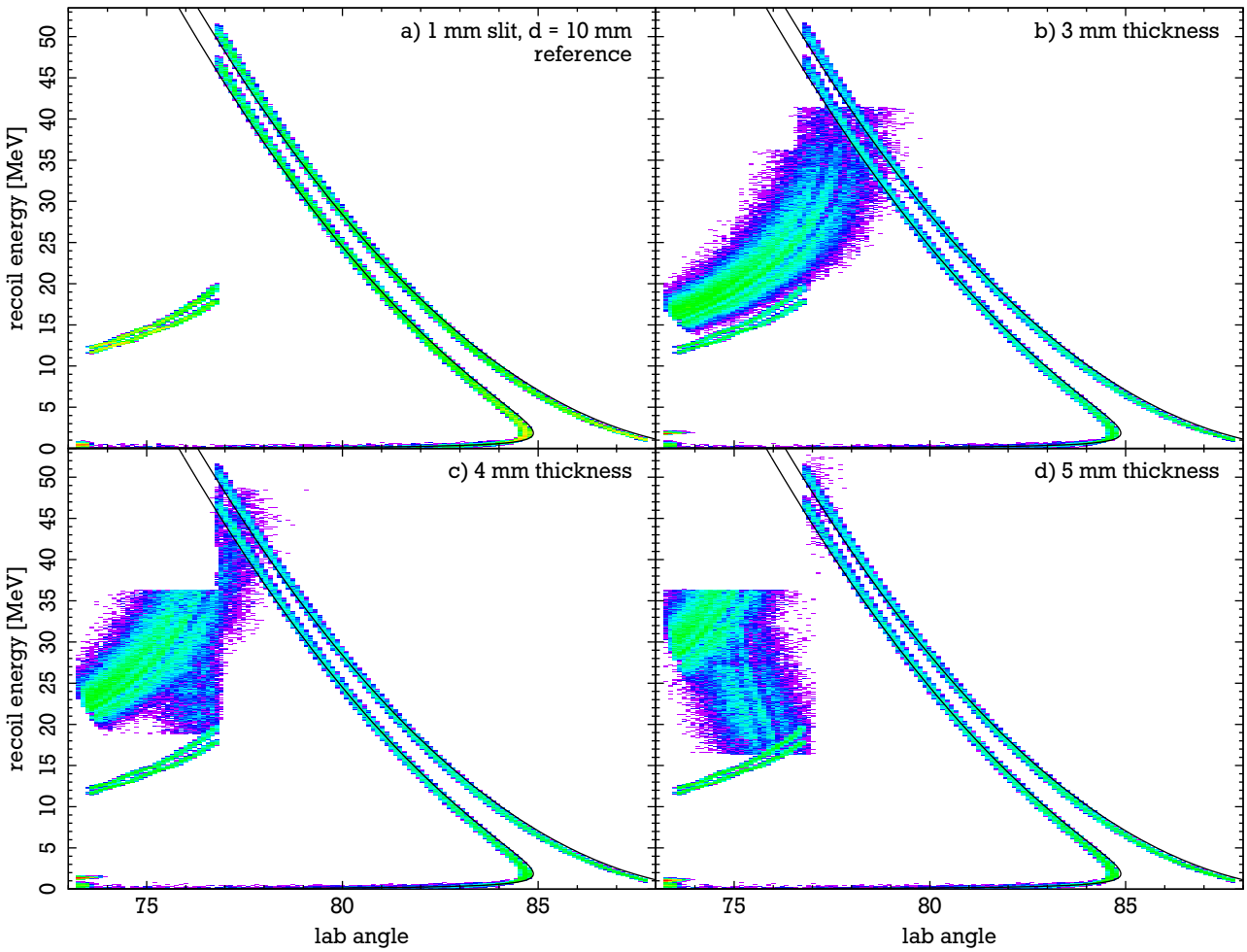

Figure 7: Simulations to determine the thickness of the slit; all simulations with a 1 mm slit at 10 mm distance

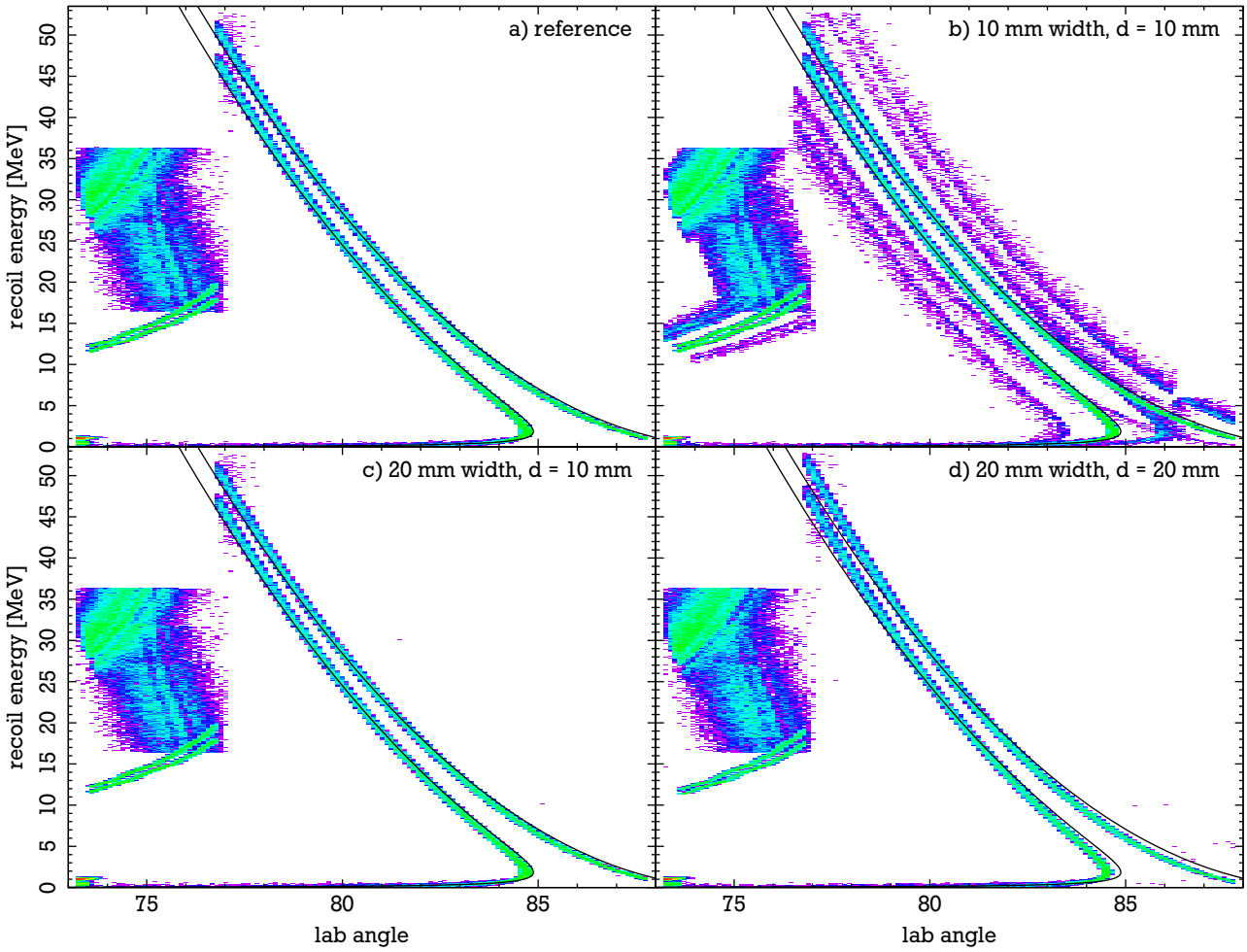

Figure 8: Simulations to determine the outer width of the slit; all simulations with a 1 mm slit, 5 mm thick at 10 mm distance

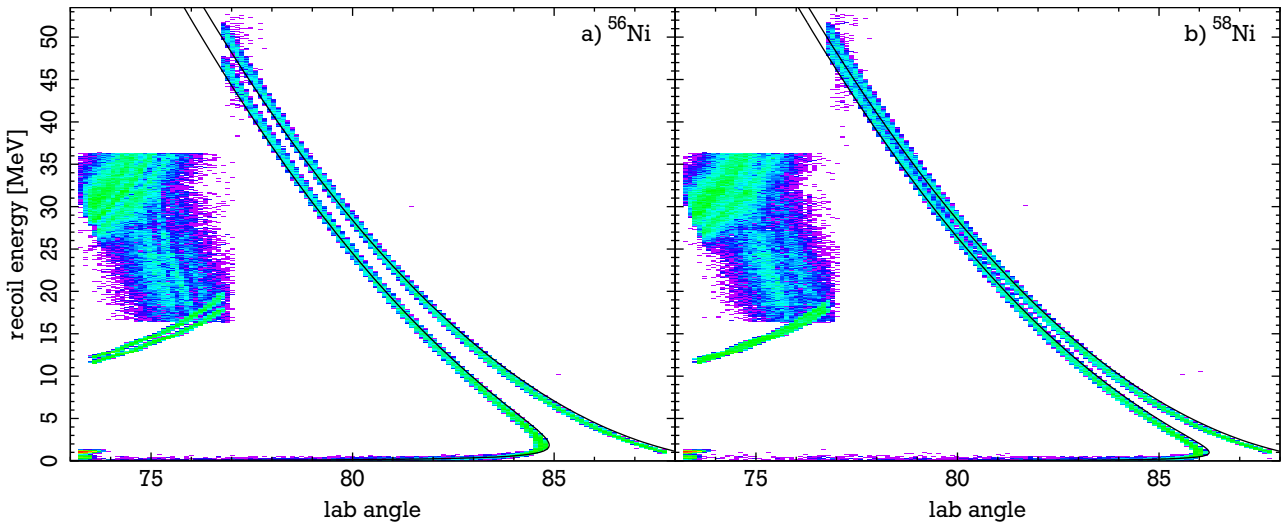

Figure 9: Slit of 1 mm, 10 mm distance, 5 mm thick Stainless steel; a) ^{56}Ni; b) ^{58}Ni

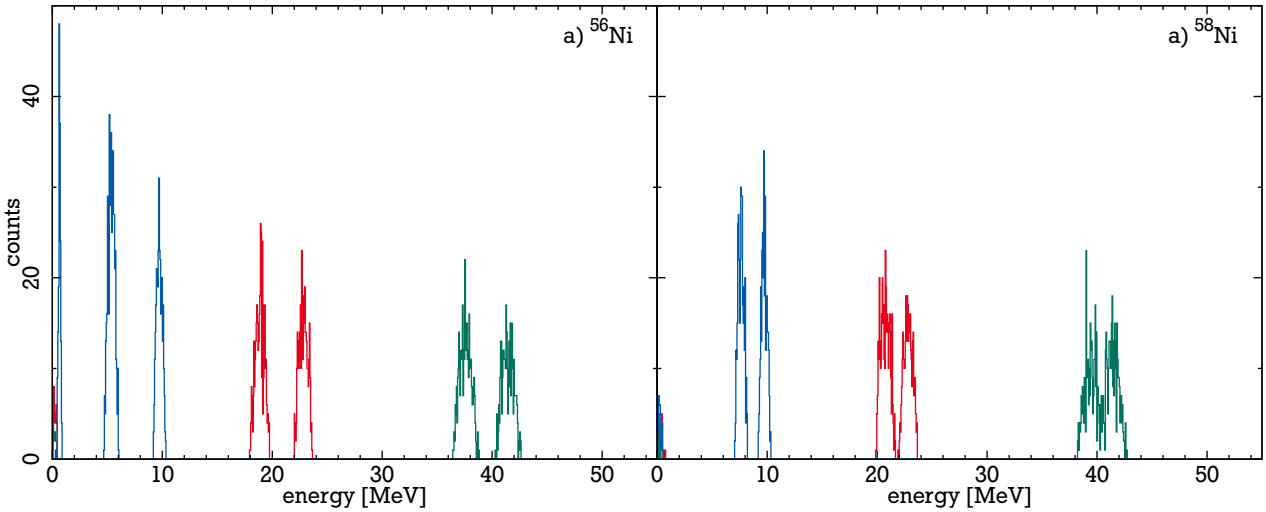

Figure 10: Cuts through the spectra of fig. 9; a) ^{56}Ni; b) ^{58}Ni; green: 78°, red: : 81°, blue: 84°

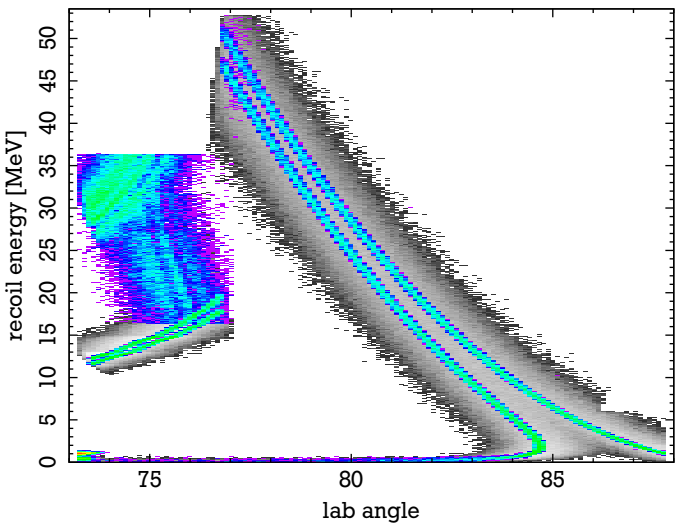

Figure 11: Final slit configuration (1 mm slit, 5 mm thickness, 10 mm distance, 20 mm width) in comparism with the pattern taken without a slit